Wip1-dependent modulation of macrophage migration and phagocytosis

Tang, Yiting; Pan, Bing; Zhou, Xin; Xiong, Kai; Gao, Qian; Huang, Lei; Xia, Ying; Shen, Ming; Yang, Shulin; Liu, Honglin; Tan, Tao; Ma, Jianjie; Xu, Xuehong; Mu, Yulian; Li, Kui

Published in:
Redox Biology

DOI:
10.1016/j.redox.2017.08.006

Publication date:
2017

Document version
Publisher's PDF, also known as Version of record

Redox Biology 13 (2017) 665–673

Contents lists available at ScienceDirect

Redox Biology

journal homepage: www.elsevier.com/locate/redox

Research paper

Wip1-dependent modulation of macrophage migration and phagocytosis

Yiting Tang[a,1], Bing Pan[b,1], Xin Zhou[c,1], Kai Xiong[d], Qian Gao[a], Lei Huang[a], Ying Xia[a], Ming Shen[e], Shulin Yang[a], Honglin Liu[e], Tao Tan[f], Jianjie Ma[f], Xuehong Xu[c], Yulian Mu[a,*], Kui Li[a,*]

[a] State Key Laboratory of Animal Nutrition, Institute of Animal Sciences, Chinese Academy of Agricultural Sciences, Beijing 100193, China
[b] The Institute of Cardiovascular Sciences and Institute of Systems Biomedicine, School of Basic Medical Sciences, and Key Laboratory of Molecular Cardiovascular Sciences of Ministry of Education, Peking University Health Science Center, Beijing 100191, China
[c] Cell Genetics and Developmental Biology, College of Life Sciences, Shaanxi Normal University, Xi'an 710062, China
[d] Department of Veterinary Clinical and Animal Sciences, University of Copenhagen, Grønnegårdsvej 7, 1870 Frederiksberg C, Denmark
[e] College of Animal Science and Technology, Nanjing Agricultural University, Nanjing 210095, China
[f] Department of Surgery, Davis Heart and Lung Research Institute, The Ohio State University, Columbus, OH 43210, United States

ABSTRACT

Macrophage accumulation within the vascular wall is a hallmark of atherosclerosis. Controlling macrophage conversion into foam cells remains a major challenge for treatment of atherosclerotic diseases. Here, we show that Wip1, a member of the PP2C family of Ser/Thr protein phosphatases, modulates macrophage migration and phagocytosis associated with atherosclerotic plaque formation. Wip1 deficiency increases migratory and phagocytic activities of the macrophage under stress conditions. Enhanced migration of *Wip1*$^{-/-}$ macrophages is mediated by Rac1-GTPase and PI3K/AKT signalling pathways. Elevated phagocytic ability of *Wip1*$^{-/-}$ macrophages is linked to CD36 plasma membrane recruitment that is regulated by AMPK activity. Our study identifies Wip1 as an intrinsic negative regulator of macrophage chemotaxis. We propose that Wip1-dependent control of macrophage function may provide avenues for preventing or eliminating plaque formation in atherosclerosis.

1. Introduction

Atherosclerosis is a chronic inflammatory disease of the vascular wall and a leading cause of death and morbidity worldwide. Macrophage plays an important role in the development of atherosclerosis [10,20,5]. An early event in atherogenesis is the adherence of monocytes to endothelial cells [17]. After transmigrating across the endothelia layer, these monocytes mature into macrophages that phagocytose lipids to become macrophage foam cells, leading to the progressive development of atherosclerotic plaques [14]. Suppression of macrophage conversion into foam cells can prevent the formation of atherosclerotic plaques. However, the knowledge gap in understanding the mechanisms that underlie the control of macrophage function in atherogenesis has been a setback in the development of novel therapies for this disease.

The wild-type p53-induced phosphatase 1 (Wip1) is a member of the PP2C family of Ser/Thr protein phosphatases that play important roles in cellular stress responses. While Wip1 was originally discovered as an oncogene by virtue of its negative control on several key tumor suppressor pathways [4,7], emerging evidence has linked Wip1 function in multiple cellular processes [15,27,29]. A recent study by Guezennec et al. showed the involvement of Wip1 in control of atherosclerosis [13]. Specifically, genetic ablation of *Wip1* resulted in suppression of macrophage conversion into foam cells by means of the ATM/mTOR signalling pathway that regulates autophagic clearance of lipid droplets in the plagues.

Many studies have established that atherosclerotic plaque regression was associated with the disappearance of foam cells caused by their emigration from plaques into regional lymph nodes [16,23]. Interventions that directly encourage macrophage departure from plaques might synergize with cholesterol-lowering therapies to more effectively treat atherosclerotic diseases [9]. In the present study, we show that Wip1 negatively regulates macrophage migration and phagocytosis during the development of atherosclerotic plaques. Macrophages lacking the expression of Wip1 displayed enhanced migration that is associated with activation of Rac1-GTPase and PI3K/AKT pathways. The enhanced phagocytic ability of *Wip1*$^{-/-}$ macrophages was regulated by AMPK activity. These findings provide a new therapeutic target for prevention or treatment of plaques in atherosclerosis.

* Corresponding authors.
E-mail addresses: mouyulian@caas.cn (Y. Mu), likui@caas.cn (K. Li).
[1] Y.T., B.P. and X.Z. contributed equally to this work.

http://dx.doi.org/10.1016/j.redox.2017.08.006
Received 7 June 2017; Received in revised form 5 August 2017; Accepted 8 August 2017
Available online 12 August 2017

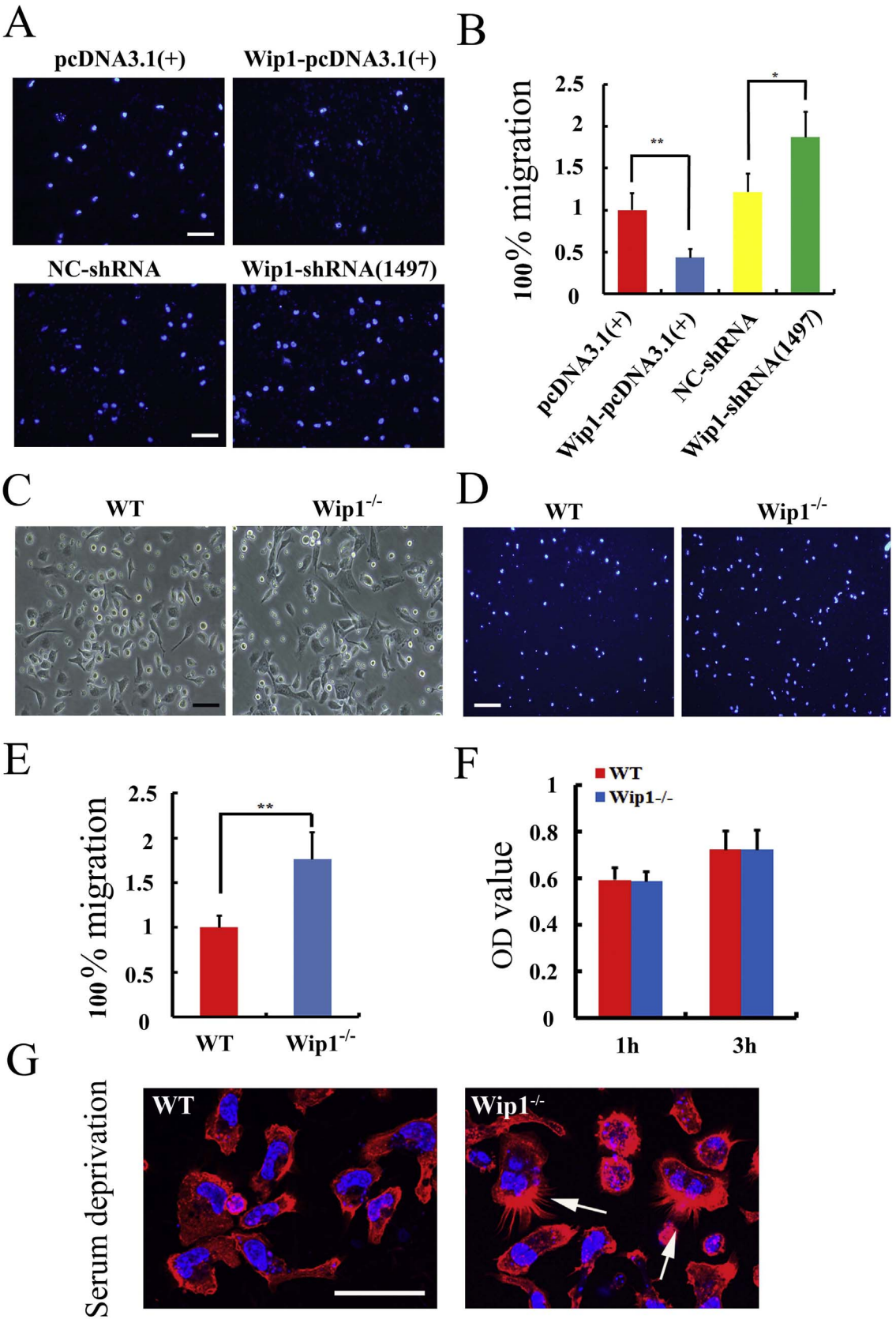

(caption on next page)

Fig. 1. *Wip1 modulates macrophage migration.* (A) Overexpression of Wip1 inhibited macrophage migration through transwell filters, whereas knockdown of Wip1 promoted migration. The migratory capacity was tested by stimulation with 10 nmol/L C5a for 3 h. Scale bars, 100 μm. (B) The results were normalized to the number of control macrophages that migrated, and are presented as the means ± SEM of 5 independent experiments performed in triplicate. *: $p < 0.05$, **: $p < 0.01$. (C) Morphology of macrophages extracted from the abdominal cavity of WT and $Wip1^{-/-}$ mice after 3 h adherence. Scale bars, 100 μm. (D) Knocking out Wip1 promoted macrophage migration through transwell filters, and the migratory capacity was tested by stimulation with 10 nmol/L C5a for 3 h. Scale bars, 100 μm. (E) The results were normalized to the number of control macrophages that migrated and are presented as the means ± SEM of 5 independent experiments performed in triplicate. **: $p < 0.01$. (F) Anchorage-dependent rate and CCK8 colourimetry measurement show that Wip1 ablation does not affect cell attachment. (G) Fluorescence confocal microscopic images of F-actin in macrophages via rhodamine-phalloidin staining. Arrows represent images of the pseudopodia structure in $Wip1^{-/-}$ macrophages. Scale bars, 20 μm.

2. Results

2.1. Wip1 negatively regulates macrophage migration and pseudopodia formation

We used J774A.1, a murine macrophage cell line [18], to examine the biological function of Wip1 in modulation of cell migration. Lipofection mediated transfection of pcDNA3.1 (*Wip1*) into J774A.1 cells led to 1.6 fold increase of Wip1 protein expression. J774A.1 cells with shRNA knockdown of Wip1 expression displayed high migratory rates compared with those transfected with a non-specific shRNA (as control). See the Supplementary Fig. 1. When Wip1 was overexpressed in J774A.1 cells, the migratory rate decreased significantly (Fig. 1A). Results from multiple experiments were summarized in Fig. 1B, and showed that macrophage migration rate negatively correlated with Wip1 protein expression.

We next used primary cells to further examine the biological function of Wip1 in modulation of cell migration. Primary peritoneal macrophages were isolated from the $Wip1^{-/-}$ and *WT* littermates and cultured by an adherence screening method [22] (Fig. 1C). Genotyping of the $Wip1^{-/-}$ mice is shown in Supplementary Fig. 2. Cell sorting using macrophage markers of CD11b and F4/80 enhanced the selection of the macrophages population in our experiments (Supplementary Fig. 3). After serum-depletion for 3 h, we found that actin in the *WT* macrophages displayed random orientations with no appreciable formation of pseudopodia. In contrast, many $Wip1^{-/-}$ macrophages appeared "polarized" and tended to form pseudopodia (Fig. 1G). We used a transwell migration assay to determine whether the pseudopodia structure is linked to altered migration of macrophages. Fig. 1F showed that there was no difference in the adhesion of macrophages between the $Wip1^{-/-}$ group and WT group, as the OD values were comparable at 1 h and 3 h under normal culture conditions. However, the migratory ability of the $Wip1^{-/-}$ group was significantly greater than the *WT* group (Fig. 1D). Compared with the WT group, the $Wip1^{-/-}$ cells displayed 76% more migratory activity ($p < 0.01$) (Fig. 1E). These data suggest that genetic ablation of Wip1 led to enhanced migratory property of the macrophages.

2.2. Knockout of Wip1 promotes macrophage migration away from inflammation

For in vivo assessment of macrophage migration, we used fluorescence labelling of primary cultured macrophages derived from the WT or $Wip1^{-/-}$ mice. WT macrophages stained positive for Light yellow (green) or $Wip1^{-/-}$ macrophages stained positive for Nile red (red) were identified with APC labelled F4/80 using FACS analysis. Equal amounts of the WT and $Wip1^{-/-}$ macrophages (6×10^4 cells each) were co-injected into the WT mice with on-going inflammation triggered by thioglycollate injection 24 h before (Fig. 2A). Three hours after injection, flow cytometry detected 1.3% of Light yellow labelled WT macrophages in the peritoneal cavity, whereas only 0.3% of Nile red-labelled $Wip1^{-/-}$ macrophages were identified under identical conditions (Fig. 2B). Similar observation was observed in two other separate experiments. Thus, $Wip1^{-/-}$ macrophages showed increased emigration from the peritoneal cavity.

Further study revealed that $Wip1^{-/-}$ promoted macrophage migration away from inflammation in vitro. As shown in Fig. 2C, when lipopolysaccharide (LPS) was added into the upper well of the transwell assay system, the $Wip1^{-/-}$ macrophages showed greater migratory activity than the WT macrophages. Conversely, when LPS was added into the lower well, the promoting effect of the *Wip1* deletion on the migration of macrophages was diminished; and the migratory activity of both WT and $Wip1^{-/-}$ cells was reduced to similar levels. The results were normalized to the number of WT control cells that migrated (Fig. 2D).

Previous studies by other investigators demonstrated that PI3K/AKT signalling was involved in cell migration [25]. To ascertain the contribution of this pathway in the $Wip1^{-/-}$ induced migration of macrophages, we dephosphorylated AKT prior to performing a transwell migration assays. We found that addition of a PI3K/AKT inhibitor, LY294002, significantly impaired WT and $Wip1^{-/-}$ macrophage migration (Fig. 2E). Statistical analyses showed that the addition of LY294002 abolished the difference in migration property of the WT and $Wip1^{-/-}$ cells (Fig. 2F). A role of AKT phosphorylation in regulating mobility of $Wip1^{-/-}$ macrophages was further assessed by western blot analysis. As shown in Fig. 2G and H, 3 h after incubation of $Wip1^{-/-}$ macrophages in serum-free media, there was significant increase the relative expression in phosphorylation of AKT at Ser473 over the WT macrophages ($p < 0.01$). This data confirmed that AKT signalling was involved in the migratory potential of macrophages.

2.3. Increased migration in $Wip1^{-/-}$ macrophage is attributable to enhanced Rac1-GTPase

Rho GTPases such as Rac, RhoA and CDC42 play crucial roles in cell migration [11]. While *Wip1* deficiency did not appear to affect the mRNA and protein expressions of Rac1, RhoA, and CDC42 (Fig. 3A and B), $Wip1^{-/-}$ macrophages displayed significant increase in Rac1-GTPase activity ($p < 0.01$) over the WT cells, whereas the activity of RhoA and CDC42 remain unchanged (Fig. 3C). Incubation of cells with NSC23766, a known inhibitor of Rac1-GTPase [8], reduced the GTPase activity in both WT and $Wip1^{-/-}$ macrophages and impaired the migratory activity of both cell groups as measured in the transwell migration assay (Fig. 3D, E). Moreover, in the presence of NSC23766, WT and $Wip1^{-/-}$ cells displayed similar migration properties, suggesting that the altered Rac1-GTPase activity is a main contributing factor for the Wip1-dependent macrophage migration.

To dissect the functional relationship between PI3K/AKT and Rac1 in Wip1-mediated macrophage migration, we performed experiments with WT and $Wip1^{-/-}$ cells using the PI3K/AKT inhibitor. As shown in Fig. 3F, incubation with NSC23766 blocked phosphorylation of AKT in both WT and $Wip1^{-/-}$ macrophages. Interestingly, the activation of Rac1 in response to C5a treatment was not suppressed by LY294002, instead was increased by 55% ($p < 0.01$) in WT macrophages (Fig. 3G). However, LY294002 has no obvious effect on Rac1 activation in $Wip1^{-/-}$ macrophages. According to these data, we speculate that Wip1 likely participate in the intermediate signalling steps between Rac1 and PI3K/AKT.

2.4. $Wip1^{-/-}$ promotes CD36 plasma membrane recruitment via activation of AMPK pathway

FACS analysis of macrophages for migration studies showed that greater numbers of $Wip1^{-/-}$ macrophages were identified to have larger

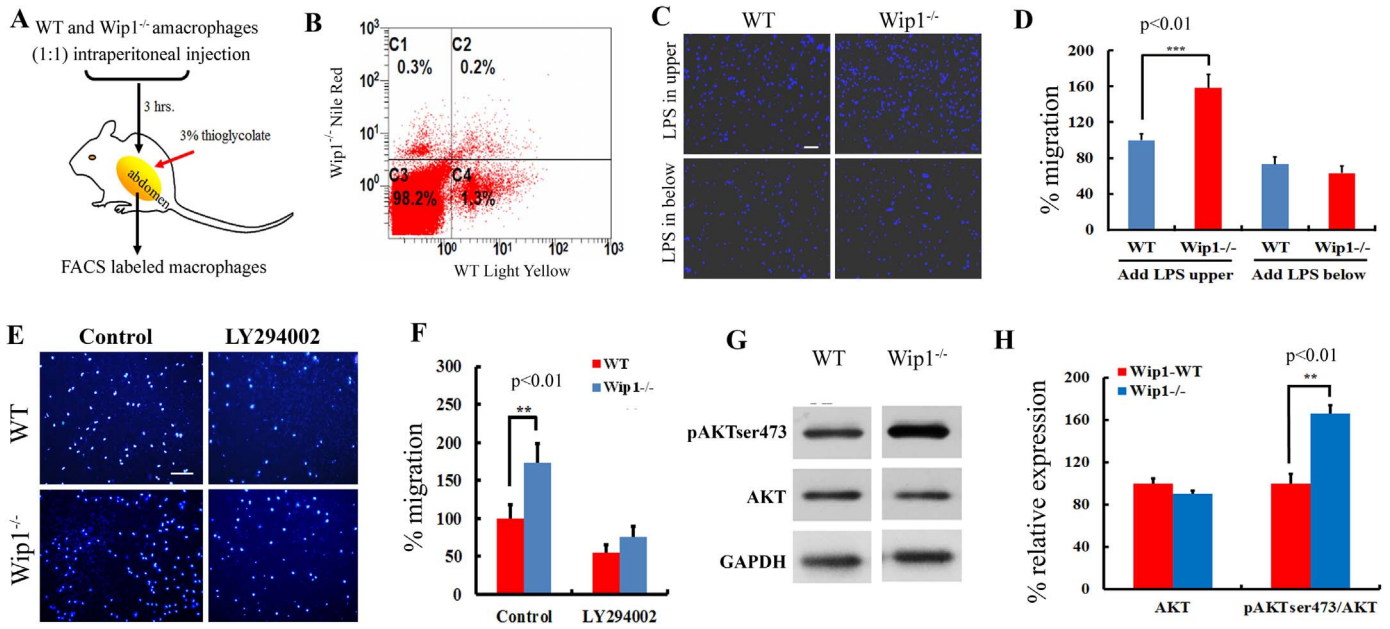

Fig. 2. *Wip1 deficiency promotes macrophage migration away from inflammation via PI3K/AKT pathways.* (A) Equal number of Nile Red labelled *Wip*$^{-/-}$ and Light Yellow labelled WT macrophages were injected into the peritoneal cavity of thioglycollate-stimulated WT mice. The amount of labelled macrophages in the cavity was analysed by FACS 3 h after the injection. (B) Flow cytometry showed more Light Yellow labelled WT macrophages remained in the peritoneum compared to Nile Red labelled *Wip1*$^{-/-}$ macrophages. Data are representative of three independent experiments. (C) The migratory capacity was tested by stimulation with 10 nmol/L C5a for 3 h. LPS was added (10 mg/L) in the upper or/and lower chamber for 3 h. Migrated macrophages were quantified after fixation and DAPI staining. Scale bars, 100 μm. (D) The results were normalized to the number of WT macrophages that migrated and are presented as the means ± SEM of 5 independent experiments performed in triplicate. ***: $p < 0.001$. (E) Macrophages from WT or *Wip1*$^{-/-}$ mice were seeded on transwell filters, and their migratory capacity was evaluated via stimulation in the presence of a PI3K/AKT inhibitor (LY294002, 50 μM) for 3 h. Migrated macrophages were quantified after fixation and DAPI staining. Scale bars, 100 μm. (F) The results were normalized to the number of WT macrophages that migrated and are presented as the means ± SEM of 5 independent experiments performed in triplicate. **: $p < 0.01$. (G) Western blot analysis of mouse macrophages. The cells were incubated in media lacking serum for 3 h. The *Wip1*$^{-/-}$cells displayed higher expression of pAKT than the WT cells. (H) Determination of the pAKT/AKT ratio after 3 h of incubation via grey-scale image analysis. The results are presented as the means ± SEM of 3 independent experiments performed in duplicate.**: $p < 0.01$.

forward scatter area compared with WT macrophages. This data suggests the possibility that *Wip1*$^{-/-}$ might enhance the phagocytotic ability of macrophages. Accordingly, we determined whether Wip1 affected the expression of specific surface molecules (CD36, CD64, CD204 and CD284) associated with phagocytosis. As shown in Fig. 4A, FACS analysis revealed that *Wip1*$^{-/-}$ promoted CD36 recruitment to macrophages. There were no significant differences in the other surface molecules (e.g. CD64, CD204 and CD284) between the WT and *Wip1*$^{-/-}$ cells. We next used western blot to assess the expression of CD36 in the cytomembrane of macrophages. As shown in Fig. 4B, following 3 h of incubation with fluorescently labelled beads and LPS (10 mg/L), *Wip1*$^{-/-}$ macrophages exhibited significantly higher level of CD36 recruitment than that of the WT macrophages. The elevated level of CD36 recruitment was sustained at 6 h of incubation ($p < 0.05$) (Fig. 4C).

Studies from other investigators have established a role for AMPK in regulation of phagocytosis [3]. We analysed the relationship between CD36 and AMPK pathways in macrophages using the AMPK specific inhibitor - compound C, and AMPK activator-AICAR. As shown in Fig. 4D and E, western blot revealed that the basal level of AMPK phosphorylation was elevated in *Wip1*$^{-/-}$ macrophages compared with that in WT macrophages ($p < 0.01$). Pre-treatment with Compound C significantly inhibited AMPK phosphorylation in *Wip1*$^{-/-}$ macrophages ($p < 0.01$), and with negligible effects on WT macrophages ($p > 0.05$). This correlates with significant reduction of CD36 recruitment in *Wip1*$^{-/-}$ cells (Fig. 4D). On the other hand, pre-treatment of cells with AICAR enhanced AMPK activation to a greater extent in WT macrophages (4.0 ± 0.5 fold) than that in *Wip1*$^{-/-}$ macrophages (1.7 ± 0.3 fold). This translates into a significant increase in CD36 levels in WT cells with treatment of AICAR, whereas a minimum increase in CD36 was observed in *Wip1*$^{-/-}$ cells following treatment with AICAR.

To further quantify the effects of Wip1 on macrophage phagocytosis, we used confocal microscopy. As shown in Fig. 5A, *Wip1*$^{-/-}$ macrophages displayed increased capacity to ingest fluorescently labelled beads compared with the WT macrophages. Statistical analysis of the confocal microscopic data showed that treatment with AICAR increased the number of labelled macrophages to similar levels in WT and *Wip1*$^{-/-}$ cells. Treatment of cells with Compound C reduced the number of labelled macrophages to similar levels in WT and *Wip1*$^{-/-}$ cells (Fig. 5B). Consistent with previous report by other investigators [1,8], we found that AMPK activation enhanced the intensity of actin staining in macrophages, predominantly in proximity to the membrane edges and the zone of filopodia, and such process could be reversed by AMPK inhibitor Compound C. Overall, our data demonstrated that the enhanced phagocytotic activity of *Wip1*$^{-/-}$ macrophages was mediated by CD36 membrane recruitment and regulated by AMPK activity.

3. Discussion

Atherosclerosis is a chronic inflammatory disease of the vascular wall, and has become a leading cause of death and morbidity worldwide. Macrophage is a key regulator of plague formation in atherosclerosis [19,30]. Using the *Wip1*$^{-/-}$ mouse model, we provide evidence that Wip1 negatively modulates macrophage migration and phagocytosis that is associated with the development of atherosclerotic plaques. Previous studies showed that selective disposal of plaques represents an efficient means for treating atherosclerosis [12]. Here we show that *Wip1* deficiency enhanced pseudopodia formation and migration of macrophages under stress conditions. Our in vivo studies showed that *Wip1*$^{-/-}$ macrophages displayed increased emigration from the peritoneal cavity. Moreover, enhanced phagocytotic activity was another signature of the *Wip1*$^{-/-}$ macrophage. Based on these data, we conclude that Wip1 functions as a negative regulator of macrophage chemotaxis. We propose that Wip1-dependent control of macrophage function may provide avenues for preventing or eliminating plaque formation in

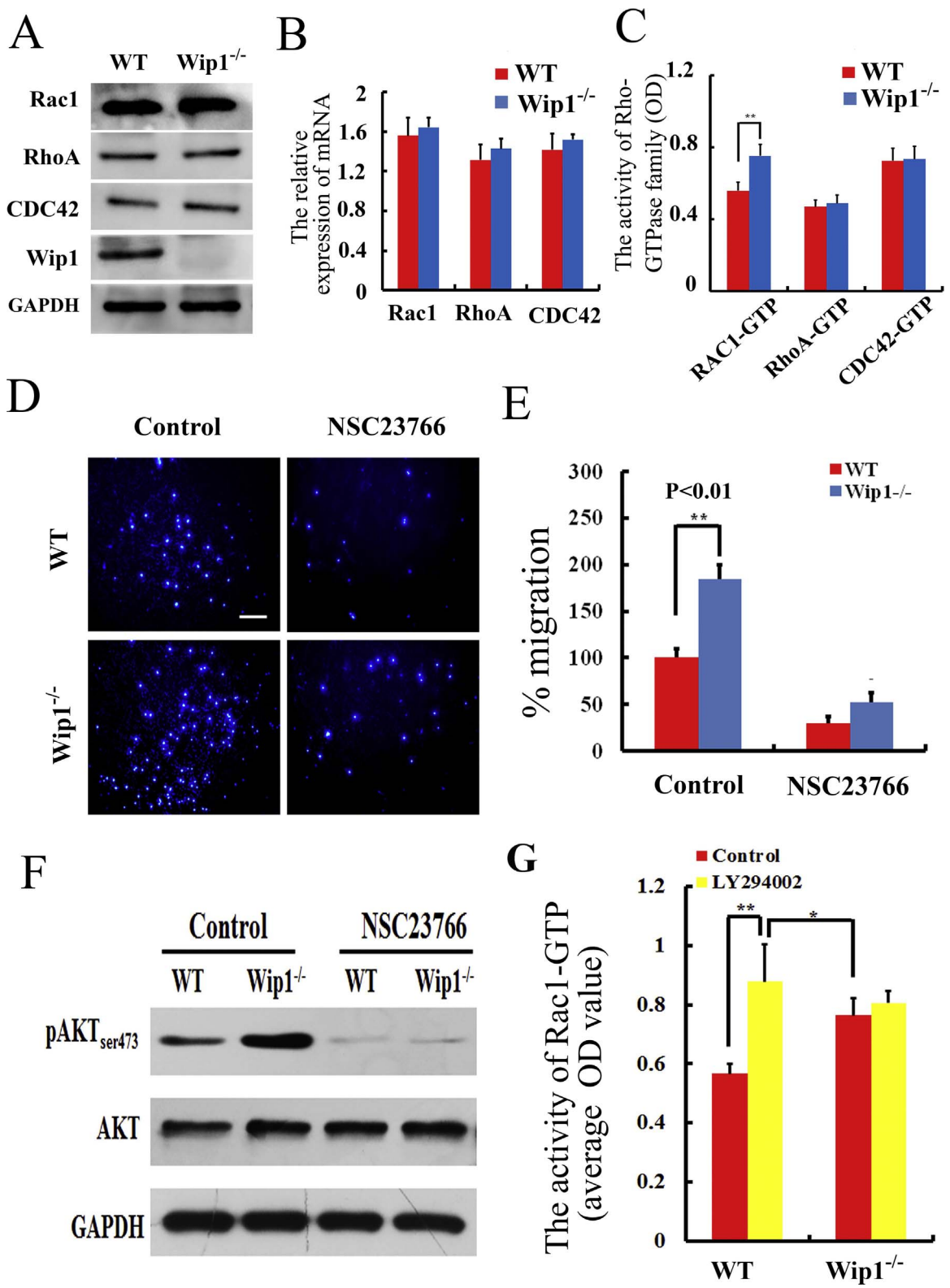

Fig. 3. *Increased migration of Wip1$^{-/-}$ macrophage is attributed to enhanced Rac1-GTPase.* (A-B) Western blot and real time PCR analysis demonstrated that Wip1 did not affect the expression of Rho family member (Rac1, RhoA, CDC42) mRNA and protein levels. (C) Knocking out *Wip1* increased the activity of Rac1-GTPase, but not RhoA and CDC42-GTPase. After the adherent macrophages were serum-depleted for 3 h, Rac1, RhoA and CDC42-GTPase activity were analysed using cell lysates and commercially available ELISA kits. The results are presented as the means ± SEM of 6 independent experiments performed in triplicate. **: $p < 0.01$. (D) Macrophages from WT or *Wip1*$^{-/-}$ mice were seeded on transwell filters (5 μm), and their migratory capacity was evaluated via stimulation in the presence of a Rac1 inhibitor (NSC23766, 100 μM) for 3 h. Migrated macrophages were quantified after fixation and DAPI staining. Scale bars, 100 μm. (E) The results were normalized to the number of WT macrophages that migrated, which are presented as the means ± SEM of 5 independent experiments performed in triplicate. **: $p < 0.01$. (F) Western blot analysis demonstrated that phosphorylation of AKT was inhibited by Rac1 inhibitor (NSC23766, 100 μM) both in the WT and *Wip1*$^{-/-}$ macrophages. (G) The results are presented as the means ± SEM of 3 independent experiments performed in duplicate.

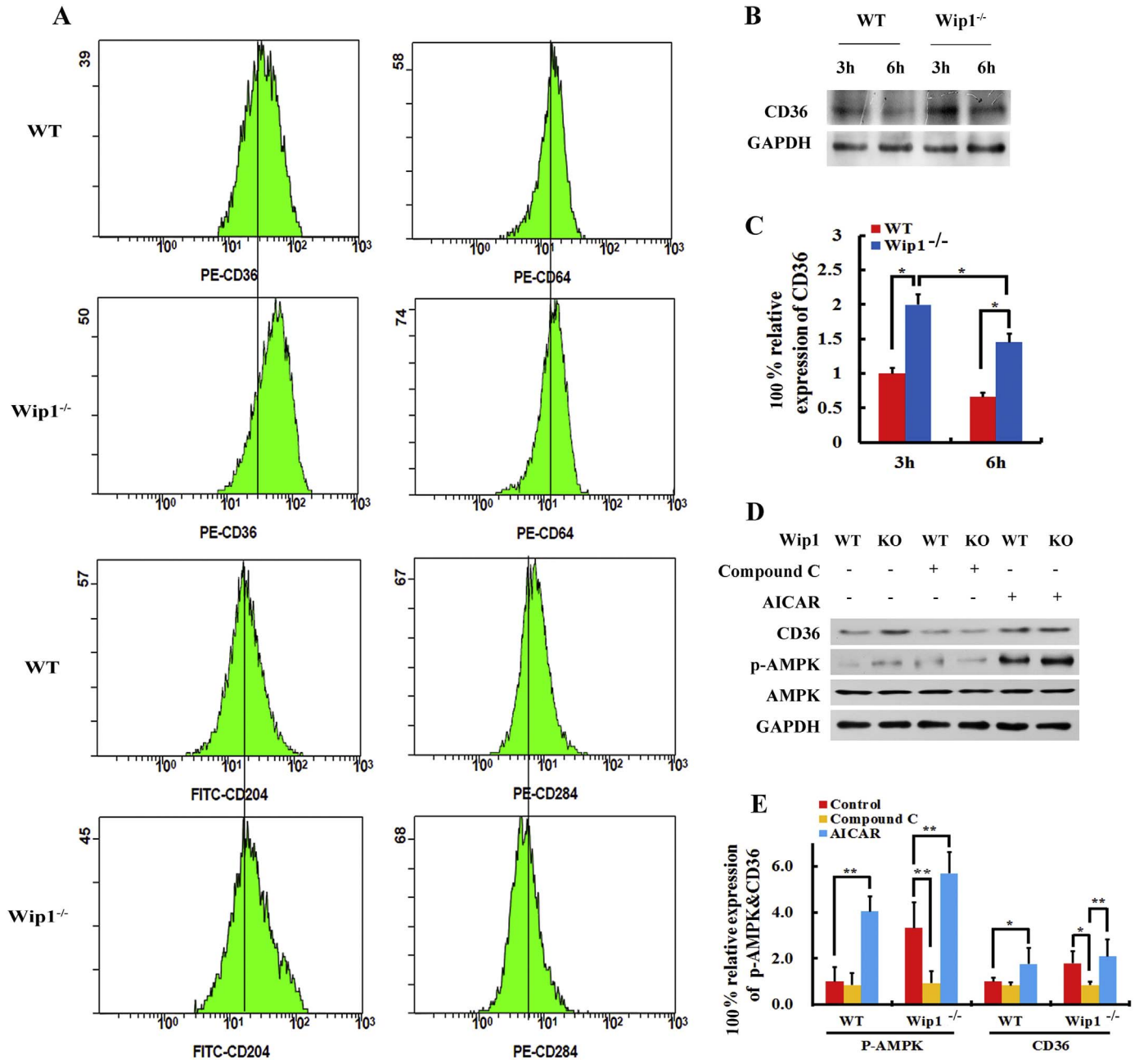

Fig. 4. *Knocking out Wip1 in macrophages promotes CD36 cytomembrane recruitment.* (A) Expression of CD36, CD64, CD204, CD284 in *WT* and *Wip1*$^{-/-}$ macrophage cytomembrane were analysed via flow cytometry. Data are representative of three independent experiments. (B) Western blot showed the expression of CD36 in WT and *Wip1*$^{-/-}$ macrophage cytomembrane. Cytomembrane recruitment of CD36 was significantly greater in *Wip1*$^{-/-}$ macrophages compared to WT after incubation with fluorescently labelled beads and LPS (100 ng/mL). (C) Determination of the CD36 relative expression ratios were shown by grey-scale image analysis. The results are presented as the means ± SEM of 3 independent experiments performed in duplicate. *: $p < 0.05$. (D) Western blot demonstrated that the expression of CD36 and pAMPK were inhibited by an AMPK pathway inhibitor (Compound C, 10 μM) and stimulated by an AMPK pathway activator AICAR (1 mM) in WT and *Wip1*$^{-/-}$ macrophages. (E) Determination of the ratio of CD36 and pAMPK relative expressions by grey-scale image analysis. The results are presented as the means ± SEM of 3 independent experiments performed in duplicate. *: $p < 0.05$, **: $p < 0.01$.

atherosclerosis.

During migration, the cells undergo polarization with extension of pseudopodia at the leading edge [26], a coordinated cellular process involving the Rho family GTPases [28]. We found that *Wip1* deficiency increased level in the active form of Rac1 GTPase and promoted the migration of macrophages. Active Rac1 at the leading edge of pseudopodia was reported to mediate actin polymerization and produce filamentous extensions and forward cell movement [21,24]. Under serum-free selection pressure, *Wip1*$^{-/-}$ macrophages displayed enhanced chemotaxis. Previous research suggested that PIP3 accumulates at the cell front in a feedback loop involving PI3K and Rac1-GTPase during chemotaxis [33]. In addition, PI3K/AKT signalling pathways are also involved in cell migration [25,32], and PI3K/AKT was reported to act both upstream and downstream of Rho-GTPases [2]. Our data suggest that the migratory ability of WT and *Wip1*$^{-/-}$macrophages was blocked by the PI3K/AKT inhibitor LY294002.

Rac1-regulated signalling can be mediated by a variety of downstream effectors [31]. By inhibiting Rac1, the phosphorylation of AKT was significantly inhibited in both *WT* and *Wip1*$^{-/-}$ macrophages. This finding indicated that Rac1 is an upstream regulatory factor of the PI3K/AKT pathway. Furthermore, results reveal that Wip1 might act as a downstream effector of PI3K/AKT in peritoneal macrophages. Thus,

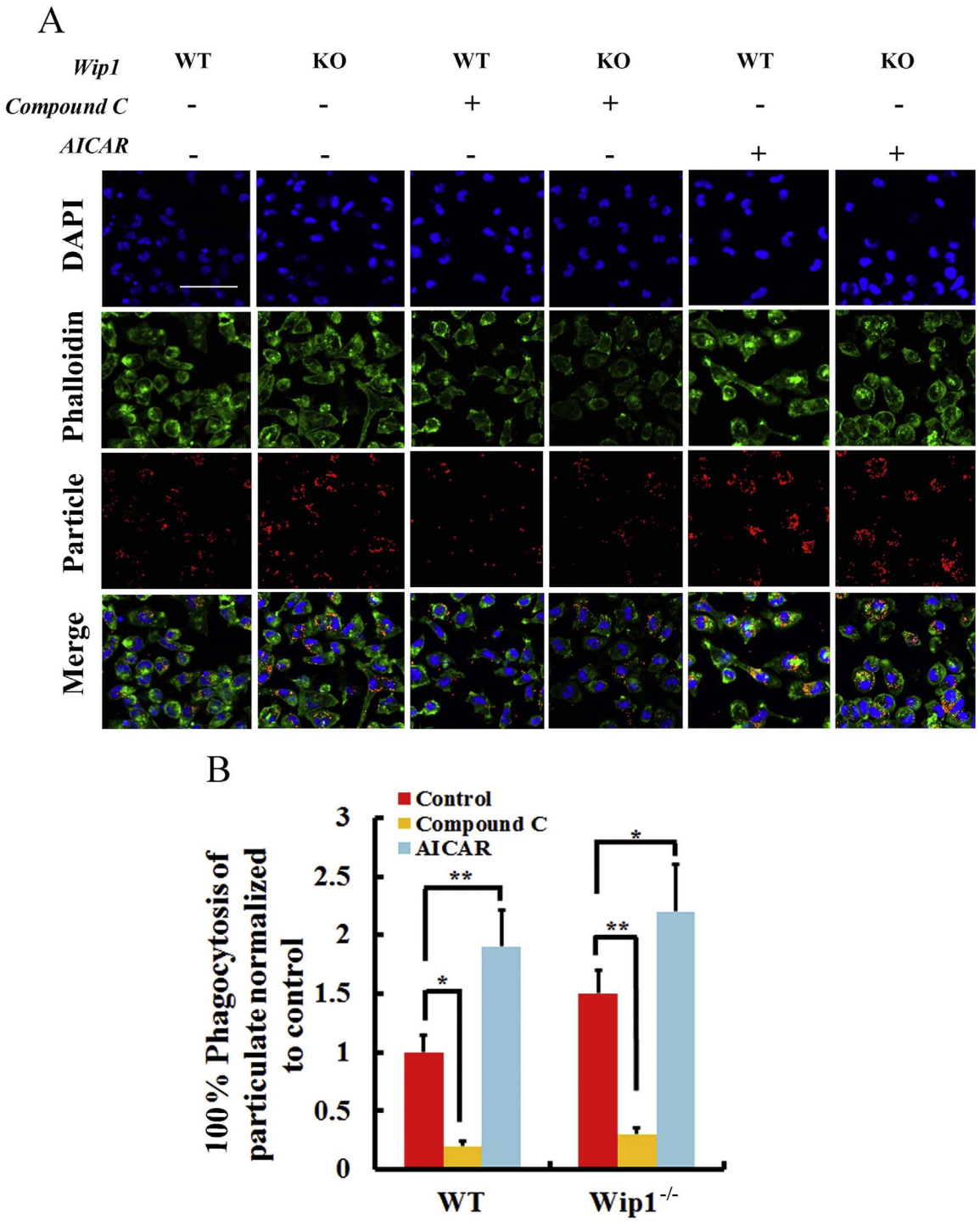

Fig. 5. *Knocking out Wip1 in macrophages promotes phagocytosis through the AMPK pathway.* (A) WT and *Wip1*$^{-/-}$ peritoneal macrophages were cultured with or without compound C (10 μM) or AICAR (1 mM). Representative fluorescence confocal microscopic images show that activation of AMPK increased, whereas compound C diminished, the uptake of fluorescent labelled beads by the WT and *Wip1*$^{-/-}$ macrophages. Green, Alex Flour-488 phalloidin; red, Nile Red fluorescent labelled particles; blue, nuclei. Scale bars, 50 μm. (B) The results were normalized to the number of control WT macrophage that phagocytosed particles, which are presented as the means ± SEM of 3 independent experiments performed in triplicate.*: $p < 0.05$, **: $p < 0.01$.

Wip1 may provide distal feedback to regulate the activation of Rac1 and the phosphorylation of AKT. Up-regulation of pAKT might be indirectly increased or stabilized by Wip1 expression.

Deletion of *Wip*1 results in the suppression of macrophage conversion into foam cells. This process appears to be independent of p53, but relies on a noncanonical ATM-mTOR signalling pathway for selective autophagy in the regulation of cholesterol efflux, thus preventing the formation of atherosclerotic plaques [13,15]. In *Wip1*$^{-/-}$ macrophages, Anna et al. also observed that mTOR kinase is down regulated through the activation of AMPK, and knocking-down TSC2 reversed the inhibitory effect of *Wip*1 deficiency on foam cell formation [3]. AMPK activation increased the ability of neutrophils or macrophages to ingest bacteria, as well as the ability of macrophages to ingest apoptotic cells [1]. Our studies indicate that Wip1 deficiency-mediated activation of AMPK increase the phagocytosis of fluorescent particles. The *Wip1*$^{-/-}$ macrophages displayed a significant increase of CD36 recruitment to

their cytomembranes. Through the use of AMPK activators and inhibitors, we demonstrate that Wip1 regulates CD36 recruitment in macrophages through the AMPK pathway.

In summary, our study supports the concept that Wip1 acts as a negative regulator of macrophage migration and phagocytosis through the Rac1-GTPase, PI3K/AKT and AMPK pathways. We propose that inhibiting the expression of Wip1 could prevent the formation of plaques, and might provide a new therapeutic target for treatment of atherosclerosis.

4. Materials and Methods

4.1. Materials

Rac1-GTP, RhoA-GTP and CDC42-GTP colorimetric ELISA kits were purchased from Cytoskeleton, Inc. FITC-CD11b and APC-F4/80 were purchased from MACS. Immunoblotting was performed using the following antibodies: Wip1 (D4F7), AKT, p-AKT (Ser473), p-AKT (Thr308), AMP-dependent protein kinase (AMPK), p-AMPK (Thr172), CD36 and GAPDH (14C10) (Cell Signalling Technology). Five-micron polycarbonate filters and 6-well culture plates were purchased from Costar. DAPI was obtained from Sigma. The rhodamine-phalloidin and Alexa Fluor® 488-phalloidin stains were purchased from Life Technologies. A Cell Counting Kit-8 (CCK8) was obtained from Dojindo Molecular Technology Corporation (Japan). Fluorescent Light Yellow and Nile Red particles (0.7–0.9 μm) were purchased from Spherotech. Bacterial LPS (LPS; *Escherichia coli* 055:B5) was purchased from Sigma-Aldrich.

4.2. Mice

Wip1$^{-/-}$ mice were kindly provided by the Key Laboratory of Human Diseases Comparative Medicine of the Ministry of Public Health (Peking, China) [6]. All mice were bred and maintained under pathogen-free conditions. Sex-matched littermate wild type (WT) mice at 8–10 weeks of age were used for the experiments, unless otherwise noted. The animal protocols were approved by the Animal Ethics Committee of the Institute of Animal Sciences in Peking, China.

4.3. Cell culture and treatment

Peritoneal macrophage cells were harvested from WT and *Wip1*$^{-/-}$ mice 24 h after receiving an intraperitoneal injection of 1 mL 3% thioglycollate. After injection of 5 mL of tissue culture medium (DMEM media, Life Technologies, USA) into the abdominal cavity, peritoneal cells were harvested. These cells were then distributed on 6-well culture plates, at a density of 2×10^6 cells/plate with DMEM media containing 10% fetal bovine serum (FBS), and incubated at 37 °C, in an atmosphere of 5% CO_2 for 2 h. Macrophages that adhered onto plates were used for further study. The murine macrophage cell line J774A.1 was purchased from Chinese Peking Union Medical College. The cells were cultured in DMEM with 10% FBS, penicillin (100 U/mL), streptomycin (100 μg/mL), and 4 mM glutamine at 37 °C.

4.4. CCK8 assay of cell adhesion

Macrophages (WT and *Wip1*$^{-/-}$) were seeded at 1×10^5 cells/well in 96-well plates with 10% serum conditions for 1 and 3 h. After 1 or 3 h, non-adherent cells were removed by washing with culture medium. Then, the number of adherent cells was measured using a CCK8 assay kit according to the manufacturer's protocol. For each well, macrophages were mixed with 10 μl of CCK-8 solution and incubated for 2 h at 37 °C. The amount of formazan dye generated by the activity of cellular dehydrogenases was measured at 450 nm using a microplate reader. Optical density (OD) values of each well represented the number of adherent cells. All experiments were performed in five replicates.

4.5. Transwell migration assay

Macrophages were seeded at a density of 1×10^5 cells on top of 5-μm polycarbonate filter inserts in transwell chamber plates (Costar). Migration capacity was determined by placing filter inserts containing the cells into wells containing 600 μl of DMEM supplemented with 10% FBS, 10% Glutamax I (Gibco) and 10 nmol/L C5a. Migration was allowed to proceed for 3 h at 37 °C in a 5% CO_2 incubator. After incubation, the filters were fixed with 4% paraformaldehyde, and cells that had not migrated were removed from the upper surface of the filter by scraping using premium quality soft cotton buds. Filters were then stained with 1 μl/mL Hoechst (Beyotime), washed with PBS, and subsequently observed under a fluorescence microscope (Nikon). Filters were visualized using a 20× objective, and the number of cells that had migrated across filters was counted at the bottom of each filter in at least 9 random fields.

4.6. In vivo migration

For in vivo migration experiments, fluorescence labelled beads (Light yellow or Nile red) (250 μl of 40 μl beads in 1 mL sterile phosphate buffer saline) were injected into the peritoneal cavity of 24-h post-thioglycollate stimulated mice (WT or *Wip1*$^{-/-}$). Three hours later, cells were isolated from the peritoneal cavity and stained for the macrophage marker F4/80. Using FACS, macrophages staining positively for Light yellow (green) or Nile red (red) were identified with APC labelled F4/80 and sorted (BD FACSAria Cell Sorter). Subsequently, equal amounts of cells positive for beads and F4/80 labelled macrophages were re-injected into mice with ongoing inflammation triggered by thioglycollate injection 24 h before. Three hours later, remaining numbers of labelled macrophages were determined by FACS as a percentage of total macrophages.

4.7. F-actin staining

Macrophages were cultured on coverslips for 24 h, incubated in media lacking FBS for 3 h or 6 h, and then fixed with 4% paraformaldehyde in the presence of 1 U/mL rhodamine-phalloidin for 30 min at room temperature. Then, coverslips were mounted on slides and observed using an Axioskop 3-channel confocal microscope (Zeiss710). Images were obtained via z-scanning and were analysed using Zen2010 software. At least three separate fields from triplicate wells were analysed per experiment for each genotype.

4.8. Assay of Rac1-GTPase activity

Macrophages were cultured in 6-well plates for 48 h in growth media, followed by incubation in DMEM (lacking FBS) for another 6 h. Then, the cells were lysed in lysis buffer, and the Rac1-GTP, RhoA-GTP and CDC42-GTP levels were measured according to the manufacturer's instructions (Cytoskeleton, Inc.).

4.9. In vitro phagocytosis assay

Phagocytosis of fluorescently labelled beads was determined by adding a 10-fold excess of fluorescent beads (0.7–0.9 μm diameter size) to a cell climbing piece. To measure the internalization of beads, they were incubated with macrophages for 3 h at 37 °C, and cells were then washed 3 times within ice-cold PBS. After fixing in 4% paraformaldehyde for 30 min and permeabilizing using 0.5% Triton X-100 for 10 min, the cells were incubated in Alexa Fluor 488-phalloidin (Green) for 30 min at room temperature. DAPI counterstaining was performed for 20 min to visualize the DNA. Fluorescence was detected using an Axioskop 3-channel confocal microscope (Zeiss710), and the fluorescence intensity was quantified using Image J software. Amounts of fluorescent beads/cell were calculated using IP-lab software. At least

three separate fields from triplicate wells were analysed per experiment for each genotype.

4.10. Statistical analysis

All data are presented as the means ± standard deviation (SD). Statistical significance was determined using the Bonferroni post-hoc test and/or Student's *t*-test; $p < 0.01$ was considered to be statistically significant.

Funding

This work was supported by Major National Scientific Research Projects (2015CB943100), National Natural Science Foundation of China (31330074, 31572378, 31272404), the National High Technology Research and Development Program of China (2012AA020603), Agricultural Science and Technology Innovation Program (ASTIP-IAS05), and the National Institutes of Health (R01AR070752).

Conflict of interest

None delared.

Acknowledgements

The authors would like to thank Lan Liu and Yang Liu of our laboratory for technical assistance.

Appendix A. Supplementary material

Supplementary data associated with this article can be found in the online version at http://dx.doi.org/10.1016/j.redox.2017.08.006.

References

[1] H.B. Bae, J.W. Zmijewski, J.S. Deshane, et al., AMP-activated protein kinase enhances the phagocytic ability of macrophages and neutrophils, Faseb J. 25 (2011) 4358–4368.
[2] D. Bar-Sagi, A. Hall, Ras and Rho GTPases: a family reunion, Cell 103 (2000) 227–238.
[3] A. Brichkina, D.V. Bulavin, WIP-ing out atherosclerosis with autophagy, Autophagy 8 (2012) 1545–1547.
[4] M.C. Buss, M. Remke, J. Lee, et al., The WIP1 oncogene promotes progression and invasion of aggressive medulloblastoma variants, Oncogene 34 (2015) 1126–1140.
[5] G. Chinetti-Gbaguidi, S. Colin, B. Staels, Macrophage subsets in atherosclerosis, Nat. Rev. Cardiol. 12 (2015) 10–17.
[6] J. Choi, B. Nannenga, O.N. Demidov, et al., Mice deficient for the wild-type p53-induced phosphatase gene (Wip1) exhibit defects in reproductive organs, immune function, and cell cycle control, Mol. Cell. Biol. 22 (2002) 1094–1105.
[7] A. Emelyanov, D.V. Bulavin, Wip1 phosphatase in breast cancer, Oncogene 34 (2015) 4429–4438.
[8] Y. Gao, J.B. Dickerson, F. Guo, et al., Rational design and characterization of a Rac GTPase-specific small molecule inhibitor, Proc. Natl. Acad. Sci. USA 101 (2004) 7618–7623.
[9] G.K. Griffin, A.H. Lichtman, Why don't macrophages leave atherosclerotic lesions? Circ. Res 110 (2012) 1273–1275.
[10] T. Gui, A. Shimokado, Y. Sun, et al., Diverse roles of macrophages in atherosclerosis: from inflammatory biology to biomarker discovery, Mediat. Inflamm. 2012 (2012) 693083.
[11] G.E. Jones, Cellular signaling in macrophage migration and chemotaxis, J. Leukoc. Biol. 68 (2000) 593–602.
[12] M.H. Kim, H.J. Kim, N.N. Kim, et al., A rotational ablation tool for calcified atherosclerotic plaque removal, Biomed. Micro. 13 (2011) 963–971.
[13] Le, X. Guezennec, A. Brichkina, Y.F. Huang, et al., Wip1-Dependent Regulation of Autophagy, Obesity, and Atherosclerosis, Cell Metab. 16 (2012) 68–80.
[14] P. Libby, Inflammation in atherosclerosis, Arterioscler., Thromb., Vasc. Biol. 32 (2012) 2045–2051.
[15] G.W. Liu, X. Hu, B. Sun, et al., Phosphatase Wip1 negatively regulates neutrophil development through p38 MAPK-STAT1, Blood 121 (2013) 519–529.
[16] J. Llodra, V. Angeli, J. Liu, et al., Emigration of monocyte-derived cells from atherosclerotic lesions characterizes regressive, but not progressive, plaques, Proc. Natl. Acad. Sci. USA 101 (2004) 11779–11784.
[17] J. Mestas, K. Ley, Monocyte-Endothelial Cell Interactions in the Development of Atherosclerosis, Trends Cardiovas Med. 18 (2008) 228–232.
[18] A. Mohammadi, A. Gholamhoseyniannajar, M.M. Yaghoobi, et al., Expression levels of heat shock protein 60 and glucose-regulated protein 78 in response to trimethylamine-N-oxide treatment in murine macrophage J774A.1 cell line, Cell Mol. Biol. 61 (2015) 94–100.
[19] K.J. Moore, I. Tabas, Macrophages in the Pathogenesis of Atherosclerosis, Cell 145 (2011) 341–355.
[20] K.J. Moore, F.J. Sheedy, E.A. Fisher, Macrophages in atherosclerosis: a dynamic balance, Nat. Rev. Immunol. 13 (2013) 709–721.
[21] C.D. Nobes, A. Hall, Rho, Rac, and Cdc42 Gtpases Regulate the Assembly of Multimolecular Focal Complexes Associated with Actin Stress Fibers, Lamellipodia, and Filopodia, Cell 81 (1995) 53–62.
[22] T.A. Pagler, M. Wang, M. Monda, et al., Deletion of ABCA1 and ABCG1 Impairs Macrophage Migration Because of Increased Rac1 Signaling, Circ. Res 108 (2011) 194–200.
[23] Y.M. Park, M. Febbraio, R.L. Silverstein, CD36 modulates migration of mouse and human macrophages in response to oxidized LDL and may contribute to macrophage trapping in the arterial intima, J. Clin. Invest 119 (2009) 136–145.
[24] R.J. Petrie, K.M. Yamada, At the leading edge of three-dimensional cell migration, J. Cell Sci. 125 (2012) 5917–5926.
[25] Y. Qian, X. Zhong, D.C. Flynn, et al., ILK mediates actinfilament rearrangements and cell migration and invasion through PI3K/Akt/Rac1 signaling, Oncogene 24 (2005) 3154–3165.
[26] M. Raftopoulou, A. Hall, Cell migration: rho GTPases lead the way, Dev. Biol. 265 (2004) 23–32.
[27] K.J. Simpson, L.M. Selfors, J. Bui, et al., Identification of genes that regulate epithelial cell migration using an siRNA screening approach, Nat. Cell Biol. 10 (2008) 1027–1038.
[28] S.T. Sit, E. Manser, Rho GTPases and their role in organizing the actin cytoskeleton, J. Cell Sci. 124 (2011) 679–683.
[29] B. Sun, X. Hu, G. Liu, et al., Phosphatase Wip1 Negatively Regulates Neutrophil Migration and Inflammation, J. Immunol. 192 (2014) 1184–1195.
[30] J.M. van Gils, M.C. Derby, L.R. Fernandes, et al., The neuroimmune guidance cue netrin-1 promotes atherosclerosis by inhibiting the emigration of macrophages from plaques, Nat. Immunol. 13 (2012) 136–143.
[31] L. VanAelst, C. DSouzaSchorey, Rho GTPases and signaling networks, Gene Dev. 11 (1997) 2295–2322.
[32] F. Wang, M. Yamauchi, M. Muramatsu, et al., RACK1 Regulates VEGF/Flt1-mediated Cell Migration via Activation of a PI3K/Akt Pathway, J. Biol. Chem. 286 (2011) 9097–9106.
[33] K. Wilson, A. Lewalle, M. Fritzsche, et al., Mechanisms of leading edge protrusion in interstitial migration, Nat. Commun. 4 (2013) 2896.